Werk

Jahr: 1980
Kollektion: fid.geo
Signatur: 8 Z NAT 2148:47
Digitalisiert: Niedersächsische Staats- und Universitätsbibliothek Göttingen
Werk Id: PPN1015067948_0047
PURL: http://resolver.sub.uni-goettingen.de/purl?PPN1015067948_0047

LOG Id: LOG_0044
LOG Titel: The evolution of the lithosphere at the Southeast flank of Reykjanes Ridge from surface wave data
LOG Typ: article

Übergeordnetes Werk

Werk Id: PPN1015067948
PURL: http://resolver.sub.uni-goettingen.de/purl?PPN1015067948
OPAC: http://opac.sub.uni-goettingen.de/DB=1/PPN?PPN=1015067948

Contact

Niedersächsische Staats- und Universitätsbibliothek Göttingen
Georg-August-Universität Göttingen
Platz der Göttinger Sieben 1
37073 Göttingen
Germany
Email: gdz@sub.uni-goettingen.de

J. Geophys. 47, 271–277, 1980

Journal of Geophysics

The Evolution of the Lithosphere at the Southeast Flank of Reykjanes Ridge From Surface Wave Data

W.R. Jacoby[1] and N. Girardin[2]

[1] Institut für Meteorologie und Geophysik, Universität Frankfurt, Feldbergstr. 47, D-6000 Frankfurt a.M. 1, Federal Republic of Germany

[2] Institute de Physique du Globe, 4, Place Jussieu, F-75230 Paris, Cedex 05, France

Abstract. Rayleigh wave group velocities for 15–40-s periods have been measured along paths parallel to the Reykjanes Ridge axis. They have traversed age slices of lithosphere between 0 and 20 Ma. Three groups of dispersion curves can be distinguished mainly on the basis of their shapes: for age slices 0–3, 6–8, and 10–20 Ma. The latter group of curves has also a significantly higher average level. Since the group velocity determinations at individual periods for anyone earthquake are not statistically independent, but the individual curves of each group are rather shifted along the velocity scale, we know their average shape better than their average level. This allows a fairly detailed resolution of vertical structure in the evolving lithosphere, particularly of S wave velocity, but only less precise information about the evolution of the absolute S velocities. Modelling has been carried out with the usual assumption of horizontal layering. A low-velocity layer with top at about 60 km depth develops with age as the lid increases its S velocities. One of the most interesting results is the suggestion of a low-velocity zone between 20 and 30 km depth; it is not yet clearly evident at 0–3 Ma age, it is distinct at 6–8 Ma age, and it appears to decay again for older age. The interpretation involves extensive melting of a peridotite mantle beneath the ridge axis; while upward segregation of melt and its drainage in the volcanic zone forms the crust, some melt may be trapped below the young thin cool lid after a few million years of age. A depleted lower high-velocity layer is left behind; it forms the lower lithosphere. Such a process will produce a chemically layered lithosphere which may be also evident at greater ages.

Key words: Lithosphere evolution – Rayleigh wave dispersion – Reykjanes Ridge.

Introduction

Rayleigh wave group velocities are used in this study to learn more about the development of the lithosphere as it is generated at the Reykjanes Ridge axis. Surface waves from earthquakes at the Charlie-Gibbs fracture zone and the southern Reykjanes Ridge travel nearly parallel to the ridge axis to the WWSSN station of Akureyri (AKU) in Northern Iceland. They sample different age slices of the lithosphere (Fig. 1).

The present paper is an extension of an earlier one (Girardin and Jacoby 1979; henceforth called 'paper I') where we treated the same data from a somewhat different point of view. Treating each group velocity determination at any period for any earthquake as statistically independent led to rather wide error bounds. We could distinguish only two groups of dispersion curves for paths through 0–8 and 10–20 Ma old lithosphere. We then attempted to interpret them with the aid of theoretical dispersion curves computed for horizontally layered models where we varied systematically three parameters and accepted all models which gave dispersion curves within the wide error bounds. We could not resolve much vertical structure. All we could detect about lithosphere evolution from 0–8 to 10–20 Ma was an increase in average S velocity in the upper 60 km from 4.2 or 4.3 km/s (and no obvious low-velocity layer) to 4.5 or 4.6 km/s (with a significant low-velocity layer underneath).

The reason for extending the study is that it is justified to look at the data accuracy more optimistically than in paper I, if one does not take the individual group velocity determinations as statistically independent. As shown below, the shapes of the dispersion curves are, actually, better known and one can, in fact, distinguish three groups by lithospheric age of the paths (through 0–3, 6–8, and 10–20 Ma old lithosphere). Consequently vertical structure and evolution with age can be resolved in more detail. This in turn sheds new light on thermodynamic and petrologic models of the evolving lithosphere at the Reykjanes Ridge.

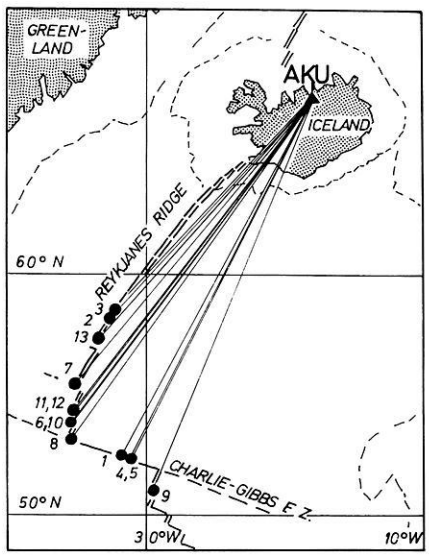

Fig. 1. Map of North Atlantic showing earthquake epicentres and station used (AKU), as well as great circle paths of Rayleigh waves between them

0340-062X/80/0047/0271/$01.40

Table 1. Earthquake parameters

No.	Date	Origin time	Coordinates (degrees)	Depth (km)	Distance (degrees)	*N*
1	July 3, 1965	02 22 18.2	52.73N 32.05W	30	14.8	107
2	September 20, 1969	00 56 52.0	58.19N 32.05W	36	9.9	83
3	September 20, 1969	01 07 42.1	58.29N 32.03W	61	9.9	113
4	September 24, 1969	03 58 58.0	52.61N 32.01W	28	14.9	162
5	September 24, 1969	04 20 51.3	52.64N 31.83W	18	14.8	172
6	January 31, 1970	16 35 03.9	53.77N 35.51W	33	14.7	143
7	April 26, 1970	06 39 54.0	55.55N 35.18W	59	13.1	130
8	August 23, 1970	11 07 18.8	53.11N 35.14W	33	15.2	128
9	September 18, 1970	16 12 08.0	51.03N 29.56W	43	15.8	189
10	September 8, 1971	20 32 30.0	53.93N 35.31W	27	14.6	89
11	April 3, 1972	18 52 59.8	54.28N 35.14W	32	14.2	242
12	April 3, 1972	20 36 22.2	54.33N 35.20W	13	14.2	247
13	June 19, 1972	06 00 51.1	57.37N 33.43W	37	11.1	169

N is the number of stations reporting for epicenter determination

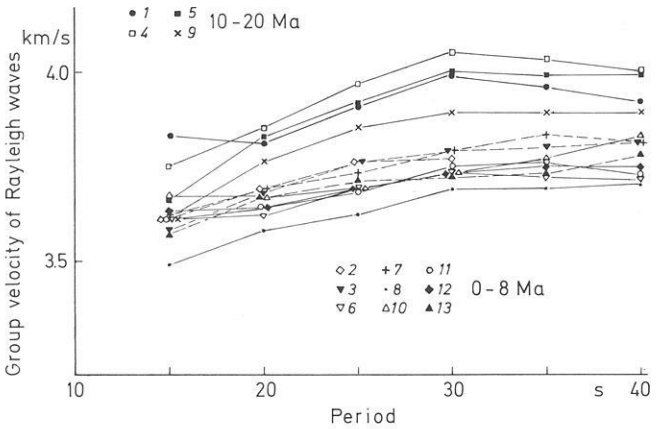

Fig. 2. Rayleigh wave group velocities measured for the 13 earthquakes shown in Fig. 1, plotted versus period (after paper I)

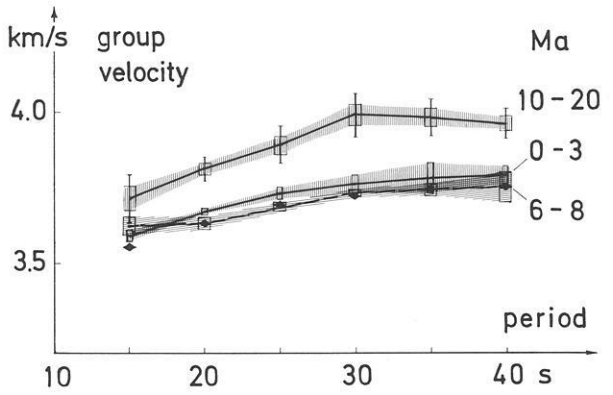

Fig. 3. Group velocities averaged for three age groups. Hatched bands correspond to the error bounds chosen for modelling

Data

Before coming to the new analysis we must briefly repeat from paper I the essential facts about the data used. Table 1 presents the earthquakes, their locations are shown in Fig. 1. The ages of the oceanic paths are taken from Heirtzler et al. (1966, 1968) and Talwani et al. (1971). The long-period records of AKU were digitized, the vertical component was analized by multiple filtering (Dzievonski et al. 1969); the group velocities for each earthquake were computed from the arrival times of maximum energy in a moving frequency window (corrected for instrumental group delay) and the source time and distance.

The results are shown in Fig. 2. All individual dispersion curves essentially rise in the 15 to 40 s period range from 3.7 to 4 km/s (10–20 Ma paths) or from 3.6 to 3.8 km/s (0–8 Ma paths); they group at two different velocity levels. In the 'older' group all curves are very similar (with one exception at 15 s) rising monotonously to 30 s and then levelling off or actually dropping. If the curves are shifted along the velocity axis they can be made to fit quite closely. There are several ways of doing this, but with only four dispersion curves at hand, it hardly matters which way is taken to estimate the best average shape. We have simply taken the arithmetic mean at each period; for the error bounds as related to shape only, we have taken half the standard deviation at each period (Fig. 3), implying that over 80% of it is related to uncertainty of velocity level.

The 'younger' group of Fig. 2 of nine dispersion curves for the age slice 0–8 Ma does not show, at first glance, much more structure than a nearly linear increase with period. Examining the curves more carefully, one notices, however, two sub-groups with different shapes; they are marked in Fig. 2 by dashed lines and by solid lines and correspond to the age slices 0–3 and 6–8 Ma, respectively. Again we have estimated their average shapes by taking the arithmetic mean at each period (Fig. 3). The standard error bands at each period are rather narrow; although they comprise both the scatter in level and random errors at each period, we accept the standard errors as the error bounds for later modelling. These error bounds do not overlap for the two sub-groups between 20 and 30 s period, but it would be difficult to argue on this basis for a very significant difference in velocity level. In shape, however, the difference appears to be more significant at the lower period end with the 0–3 Ma curve rising monotonously

and the 6–8 Ma curve showing a clear dip if not a weak actual minimum at 20 s.

For the assessment of the significance of the data it is important to discuss briefly the errors of the group velocity determinations. For more details the reader is referred to paper I. Errors of the earthquake source parameters, particularly latitude, depth, and origin time will mainly shift the dispersion curves along the velocity axis, a type of scatter in fact observed. The focal depths given in Table 1 (from ISC) are probably in most cases too great (Weidner and Aki 1973); if this is so, the group velocities, particularly for the 0–3 Ma age slice, could be lower by 1%, or so, than given in Figs. 2 and 3; this would reduce the difference in level between the 0–3 and the 6–8 Ma groups. Very small focal depths also lessen the uncertainty of initial phase which is independent from frequency for any focal mechanism at zero depth. We have, nevertheless refrained from using phase velocities which could still be critically affected by the unknown initial phase related to the unknown focal mechanisms.

There are other effects hampering the interpretation. The possibility of lateral refraction along paths particularly near the ridge axis cannot be dismissed, although the polarization at AKU is close to theoretical. The result will be one of smearing out the effects of evolution with lithospheric age and thus will make us rather underestimate than overestimate them. The same can be said about the fact that the paths to some extent intersect the lithospheric isochrons and that the precise age is not everywhere known.

More serious is the uncertain influence of Iceland itself on the group velocities since the waves traverse significant distances through it. In paper I we could, however, show that the influence is not too critical to our study. (1) It is not very large in the period range considered. (2) It does not strongly depend on the various Iceland models we had tested. (3) It does not strongly depend on the different oceanic paths which closely converge on AKU in Iceland. (4) The influence does, however, subdue rather than enhance the differences between the dispersion curves for the different age groups; this last point is perhaps the most important one, because if we use the observed Rayleigh wave group velocities of paper I without the 'Iceland correction' we are not in danger of overestimating the variations related to lithospheric evolution.

Table 2. Top parts of models for Rayleigh wave group velocity computations: water depths and crustal structures

Age slice (Ma)	Depth (km)	*P* velocity (km/s)	*S* velocity (km/s)	Density (g/cm³)
0–3	0.0	1.52	0.0	1.03
		1.52	0.0	1.03
	0.9			
		2.8	1.6	2.7
		3.9	2.3	2.8
	2.3			
		4.9	3.2	2.9
	5.0	5.9	4.0	3.0
6–8	0.0	1.52	0.0	1.03
		1.52	0.0	1.03
	1.5			
		1.65	1.0	2.0
		1.65	1.0	2.0
	1.6			
		3.7	2.15	2.7
		5.3	3.1	2.8
	3.3			
		6.1	3.5	2.9
	5.5	7.3	4.1	3.0
10–20	0.0	1.52	0.0	1.03
		1.52	0.0	1.03
	2.3			
		1.65	1.0	2.0
		1.65	1.0	2.0
	2.5			
		4.7	2.7	2.6
		4.7	2.7	2.6
	4.5			
		6.3	3.6	2.9
	6.5	6.3	3.6	2.9

Velocities and densities vary linearly from top to bottom of layers

Shear Velocity Structure of Reykjanes Ridge

We use simple methods for the interpretation of the data. The uncertainties discussed in the two previous paragraphs really have to do with our incapability of modelling surface wave propagation through a complex three-dimensional structure. For the computation of theoretical dispersion curves we had to assume horizontally layered models for the three different age slices. We know that this is a very crude approximation to reality. We must, however, also economize; the kind of data we have does not warrant the application of more sophisticated cumbersome methods which would resolve more details only in connection with much more precise data.

We repeat that we are not worried about the fact that the use of horizontally layered models will 'smear out' the real lateral variation of structure with lithospheric age; so will the neglect of the influence of Iceland. We must, however, worry about unpredictable effects of the simple modelling and keep this in mind until better modelling becomes available. We warn the reader to remain aware of this.

We believe that the interesting variations of vertical structure which we do see are not grossly wrong and that they give us hints to the thermodynamic and petrologic processes involved in lithosphere generation.

In modelling we have constrained water depth and crustal structure. Table 2 states our assumptions for the three age groups; they are mainly based on *P* velocities found by Talwani et al. (1971) for the NW flank of Reykjanes Ridge, supplemented by recent results of the RRISP Working Group (1979) on the SE flank. As average structures they are not without uncertainty; To investigate what an effect an error in crustal structure and water depth may have on the theoretical dispersion curves, we did some of the model computations twice: 1. with the 'correct' water and crust of Table 2 (e.g. with the 0–3 Ma water/crust for a 0–3 Ma mantle model) and 2. with the 'wrong' one (i.e., with the 6–8 Ma water/crust for a 0–3 Ma mantle model and vice versa); the effect in the period range considered is largely one of shifting the dispersion curves.

In modelling the 0–3 and 6–8 Ma structures we also held the *S* velocity below 70 km fixed at 4.1 km/s, indicated by a heavy

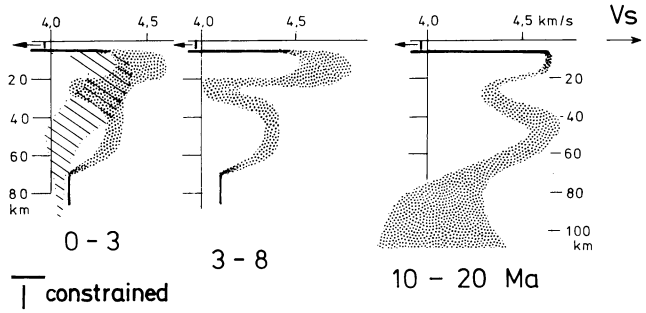

Fig. 4. Range of models found for the three age slices. *Each of the shaded areas* encompasses several models for which dispersion curves have been computed to fall within the error bounds of Fig. 3; wavelengths of vertical S velocity variation in the models has generally been held above 20 km. Regions of velocity-depth functions held fixed during modelling shown by *heavy lines*. Hatched model area in the 0–3 Ma slice is taken from Keen et al. (this volume) for comparison

line in Fig. 4 giving the modelling results. In the 10–20 Ma models the S velocities below 70 km depth were allowed to vary (Fig. 4); this will be discussed below.

The P velocities in the upper mantle were assumed to be linked to the S velocities with Poisson's ratios between 0.25 and 0.3; the densities were computed with Birch's (1960, 1961) velocity-density relationship. The effect of these assumptions on the results is only slight.

The method and the program used for computing the theoretical dispersion curves are due to Derr (1967). The program gives the eigenfunctions of spherical earth models for specified modes and thence the phase and group velocities of Rayleigh and/or Love waves.

In searching for models which give dispersion curves within the error bounds of Fig. 3, we were guided by the models presented in paper I; they had been found by a systematic search of three parameters for only two average dispersion curves (0–8 and 10–20 Ma) with wide error bounds. For the present study we used the traditional manual search by trial and error. We were, however, not content with a single acceptable model for each age group but rather repeated the search many times from different starting points. In modelling we attempted to avoid unresolvable detail by allowing the S velocity to vary only with 'vertical wavelengths' greater than 10 or 20 km, keeping in mind the trade-off between the uncertainty of average velocity determination and the (vertical) averaging distance (Backus and Gilbert 1968), but we did not strictly apply inversion theory.

The results of our search for the three age groups are presented in Fig. 4. Instead of showing the individual S velocity-depth models we found to be compatible with the observations, we only show the bands comprising all models. This does not mean that a velocity-depth function which takes an arbitrary course through such a band will necessarily give an acceptable dispersion curve; a function meandering through the band has, however, a good chance. We cannot claim that we have fully explored the extremes of the model space, but we have attempted to carefully investigate those features which appeared important to us. These are mainly the upper low-velocity layer in the 20 to 30 km depth range, particularly for the 6–8 and 10–20 Ma age slices, and the depth to the deeper and broader low-velocity layer which is commonly associated with the asthenosphere (tested mainly for 10–20 Ma).

We attempted to find models (6–8, 10–20 Ma) without an upper low-velocity channel but we were not successful, particularly if we constrained the uppermost mantle S velocities to be >4.4 km/s, according to the S_n velocities found by Hart and Press (1973). Without a high top velocity and a channel the computed dispersion curves are convex upward at the low period end; introduction of this feature brings about the correct shape. From this point of view the upper low-velocity layer must be significant in the 6–8 Ma slice to produce the dip in the dispersion curve at 20 s period. Although we found this feature without fixing the topmost mantle velocity, we probably need this constraint because other parameters as water depth and crustal structure are not known precisely enough. This uncertainty does, in fact, cause the large models scatter at shallow depth for 0–3 and 6–8 Ma (Fig. 4).

We also searched systematically for the depth to the top of the deeper, i.e., 'asthenospheric' low-velocity layer whose bottom we cannot 'see'. Attempts to place the top as shallow as 50 km or as deep as 90 km failed; the significant velocity decrease occurs at a depth of 60 or 70 km in agreement with Press (1970), Haigh (1973), and Forsyth (1977), among others. The wide scatter of the models for 10–20 Ma in this depth range reflecting the lack of resolution from 15–40 s data leaves us sufficient confidence in the 60 to 70 km top of the 'asthenosphere'. The small scatter in the 0–3 and 6–8 Ma models at depth is, of course, the result of fixing the channel velocity and of avoiding drastic short-wavelength variations directly above.

The development of the models (Fig. 4) in steps from 0–3 to 6–8 and 10–20 Ma involves a rise of the upper-lid velocity by about 0.2 km/s and the upper channel becoming pronounced at 6–8 Ma and perhaps weakening thereafter. The S velocity of the lower high-velocity layer clearly increases in the third stage. The bottom of this lower layer becomes more pronounced but its depth does not significantly change. A square-root age growth of lithospheric thickness (Parker and Oldenburg 1973) is not evident but, because the age span of our data is too short, we cannot really test this. For the 0–20 Ma span a more complicated nature of the lithospheric growth is, however, suggested. The definition of the lithosphere as one high-velocity lid may break down if both channels are 'weak' mechanically. Alternatively, if the upper lid forms the 'strong' lithosphere of about 20-km thickness for the first few million years, there may be an abrupt thickness increase at about 10 Ma of age.

A Model for Lithosphere Generated at Reykjanes Ridge

In the following discussion we attempt to give a plausible explanation for the S velocity structure presented above. The model is largely based on work by Forsyth (1977), Green and Lieberman (1976), Bottinga (1974), Bottinga and Allègre (1976) and others. We assume a predominantly peridotitic upper mantle or one that is chemically a mixture of peridotite and tholeiite basalt (Ringwood 1966) with small traces of water and adopt Green and Liebermann's (1976, Fig. 1) phase diagram for $\leqq 0.4\%$ H_2O content and $CO_2 \ll H_2O$ (Fig. 5). In Fig. 5 we also show Forsyth's (1977) geotherms (long-dashed lines) computed for a cooling half-space with heat sources in the upper 300 km. The lithosphere in this model represents a thermal boundary layer. In the age range of interest, however, there is little difference between this and the cooling slab model (e.g. McKenzie 1967, Sclater and Francheteau 1970) if equivalent boundary conditions are chosen. The solidi are then mapped into the cooling lithosphere shown in Fig. 6 as stippled bands; also shown are average S velocities in four depth intervals and three age zones taken from Fig. 4.

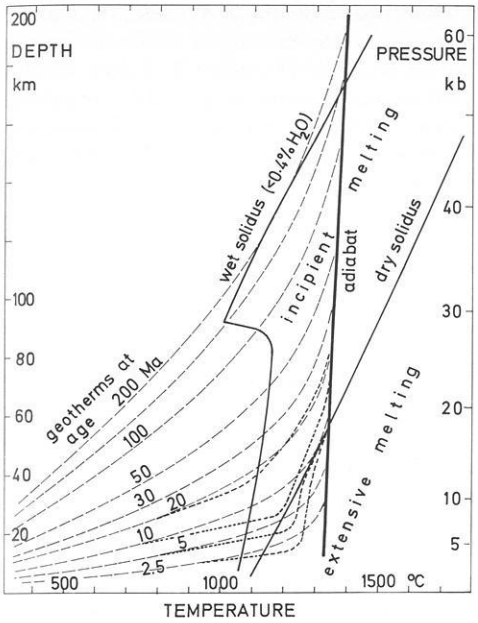

Fig. 5. Phase diagram of peridotite with 0.4% of water after Green and Liebermann (1976); geotherms after Forsyth (1977): *long-dashed lines;* qualitatively drawn distortions of geotherms, caused by two-phase convection: *short-dashed lines*

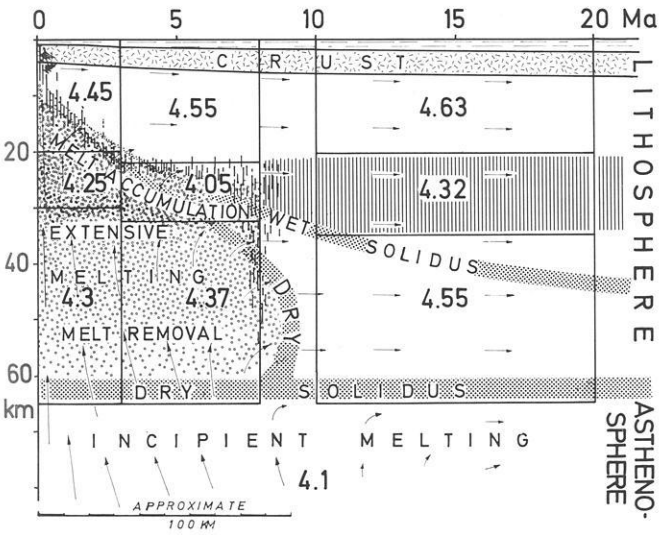

Fig. 6. Cartoon of the structure of Reykjanes Ridge based on theoretical geotherms (Forsyth 1977) and peridotite phase diagram with traces of water (Green and Liebermann 1976). *Heavy numbers* are average model *S* velocities in km/s for depth ranges shown (taken from Fig. 4). Solidi of conduction solution (Forsyth 1977): *dotted bands;* distortions of solidi by two-phase convection: bands of irregular *vertical lines. Arrows* depict flow lines qualitatively, their lengths approximately depict the flow velocities). See text for further discussion

If we now compare on Fig. 6 our *S* velocities with the solidi (stippled) taken from Forsyth, we find a fairly good agreement except in the region of the top low-velocity layer between 20 and 30 km depth at ages beyond 5 Ma or so. This suggests to us that the model for the young lithosphere should be somewhat modified. While Forsyth argued only for melt removal from, and depletion of, the lower lithosphere (to explain its apparently rapid thickening till 10 Ma, or so, and its constant thickness thereafter), we propose that we also 'see' melt accumulation near the top, forming the 20 to 30 km low-velocity zone after a few million years of cooling of the uppermost lithosphere forming a kind of 'magma-tight' lid. Melt depletion at depth and accumulation higher up might be looked upon as two-phase convection described by Frank (1968). As a consequence the geotherms would be distorted (as intuitively sketched by the short-dashed lines in Fig. 5) and so would the solidi. The resulting chemical differentiation would, however, make the application of the solidi problematical for parts of the structure. The low-velocity layer beyond 10 Ma would probably decay or could be frozen into the lithosphere as its chemical layering.

The essential features of the above picture were, in fact, predicted by quantitative petrological model calculations of Bottinga (1974), Bottinga and Allègre (1976) and Steinmetz et al. (1976). For a ridge with a half-spreading rate of 1 cm/a their models display a similar region where melt is concentrated between 20 and 30 or 40 km depth and between 10 and 50 km from the axis. The small amount of melt will cause a distinct low-velocity layer; the *S* velocity structure predicted is thus quite similar to the one we found. The distortion of the geotherms with respect to the conduction solution is also similar to the one we only guessed (Fig. 5). The upper low *P* velocity layer of Steinmetz et al. (1976) is at a slightly shallower depth than our *S* velocity channel. The physical reason for the 'asthenospheric upwelling model' of Bottinga and colleagues doing the trick explaining the *upper* low-velocity layer seems to be that it includes the two-phase convection of melt advancing from a residue.

Complimentary evidence for the top low-velocity layer has recently been presented by Yu and Mitchell (1979) who used regionalized group and phase velocities of Rayleigh and Love waves to deduce mantle shear velocities for Pacific Plate age slices of 0–20, 20–50, 50–100, and > 100 Ma. They found a 'lithospheric' low-velocity layer in the same depth range, but at older ages (20–50 Ma) than we found; they state that its existence still must be scrutinized.

Most explosion seismic studies at ocean ridges (e.g. Orcutt et al. 1976; Steinmetz et al. 1976; and many others) did not reach sufficient depth. Steinmetz et al. (1976), for a profile along the 9 Ma isochron west of the Azores, report a high velocity layer at 30 km depth which might correspond to the bottom of our proposed channel. A long-range refraction experiment along the SE flank of Reykjanes Ridge and across Iceland (RRISP Working Group, 1979; this volume; Gebrande et al., this volume) gave indirect evidence of a 'lithospheric' low-velocity channel; very low-amplitude first arrivals on Iceland from marine shots at > 200 and 400 km distance may be interpreted as indicating the shadow zone corresponding to it.

Support for an initially very thin lithosphere comes from a study of topography and gravity near the Mid-Atlantic Ridge axis (McKenzie and Bowin 1976) suggesting that the elastically bending part of the lithosphere to some distance from the ridge axis is only about 10 km thick. The value is expected to be lower than the seismic thickness. The mushroom shaped low-density body under Reykjanes Ridge of Talwani et al. (1965) also resembles our velocity model.

Further seismological support, though only in a gross sense, may be taken from the *Q* structure of the southern Reykjanes Ridge proposed by Solomon (1973) and from its *S* velocity structure assumed by Solomon and Julian (1971) to explain anomalous

fault-plane solutions. In an even cruder sense, support for low mantle velocities and partial melting below the ridge comes from the travel time residuals in the Reykjanes Ridge Iceland area for *P* waves (Francis 1969) and *S* waves (Girardin and Poupinet 1974; Duschenes and Solomon 1977).

Conclusions

Surface wave dispersion data have been interpreted to indicate a peculiar *S* velocity structure of Reykjanes Ridge with a 'lithospheric' low-velocity zone which comes into being at some distance from the axis and may then decay again. The surface wave evidence may not be totally convincing by itself, but additional seismological constraints make the interpretation plausible. The structure has then been explained by a thermodynamic-petrological model in line with Bottinga's (1974) and its extensions.

The model would, in principle, be expected to apply to all spreading ridges; but it is, of course, quite possible that the structure of Reykjanes Ridge is unique, related to the closeness of the hot spot of Iceland (Vogt and Johnson 1975). We shall, nevertheless, conclude this paper by sketching a cartoon of how we envisage the formation of the lithosphere (at Reykjanes Ridge).

Mantle material is assumed to rise adiabatically from great depth beneath the ridge axis. The mantle solidus is probably depressed to a certain extent (to the wet solidus) by water activity; the amount of partial melting will depend on the quantity of water present (Bottinga and Allègre 1978; Wyllie 1971). Thus, the material passes through a region between the wet and dry solidi in which incipient melting will occur; the melt fraction is probably too small to lead to extensive gravitational upward filtering. Above the dry solidus at ~ 60 km, melting becomes extensive, the fraction increases, and the melt will begin to buoyantly rise more rapidly through the crystal mush than the bulk moves. At depth, melt removal and crystal accumulation will prevail; this part will 'dry out' Higher up, melt will accumulate; this part will be enriched in volatiles, magma chambers will form and will tend to spill out, predominantly at thr ridge axis to form the chemically distinct crust.

The shape of the barriers to this process of two-phase convention is determined by the geotherms intersecting the wet and dry solidi. In the zone of depletion the dry solidus will mark the boundary between the 'fluid' rising asthenosphere and the 'solid' lithosphere; the wet solidus will be irrelevant here. The temperature will be lower than in the conduction case. At shallower levels where melt accumulates it will probably be the wet solidus that is important. The temperature will be higher than in the conduction case. A thin lid will nevertheless form by cooling and this will help trapping and concentrating the melt, the lid may not be perfectly magma-tight as suggested by volcanoes off the ridge axis. The effect of these processes will be to widen the rising column of asthenosphere at shallow depth and perhaps to narrow it at depth, as illustrated by Fig. 6. A mushroom shape will develop as is familiar from diapiric structures. The physical reasons, however, are quite different in both cases. In diapirs it is the bulk that spreads laterally at high levels; in our model of rising asthenosphere it is the light melt which moves faster and more steeply than the bulk before it accumulates. The resulting density structure is quite similar. But as the lithosphere spreads as a whole (in contrast to diapiric processes) it will be chemically layered. Future experiments may test this feature.

Further thorough research is needed to verify, or to decide against, our model of lithosphere generation.

Acknowledgements. Critical comments by Y Bottinga, R. Gaulon, K. v. Gehlen, S. Gregersen, S. Müller, and D. Forsyth who read an earlier version of this paper were helpful. T. Kurita supplied his version of the surface wave computer program. Computing facilities at the University of Frankfurt were used. Financial support by Deutsche Forschungsgemeinschaft grant Ja 258/6 is acknowledged. We are grateful to all of them.

References

Backus, G.E., Gilbert, F.. The resolving power of gross earth data. Geophys. J. R. Astron. Soc. **16**, 169–205, 1968

Birch, F.: The velocity of compressional waves in rocks to 10 kbars, 1. J. Geophys. Res. **65**, 1083–1102, 1960

Birch, F.· The velocity of compressional waves in rocks to 10 kbars, 2. J. Geophys. Res. **66**, 2199–2224, 1961

Bottinga, Y Thermal aspects of sea-floor spreading, and the nature of the sub-oceanic lithosphere. Tectonophysics **21**, 15–38, 1974

Bottinga, Y., Allègre, C.· Geophysical, petrological, and geochemical models of the oceanic lithosphere. Tectonophysics **32**, 9–59, 1976

Bottinga, Y., Allègre, C.J.. Partial melting under spreading ridges. Philos. Trans. R. Soc. London. Ser. A: **288**, 501–525, 1978

Derr, J.S.. A comparison of free oscillations of oceanic and continental earth models. Bull. Seismol. Soc. Am. **57**, 1047–1061, 1967

Duschenes, J.D., Solomon, S.C.. Shear wave travel time residuals from oceanic earthquakes and the evolution of oceanic lithosphere. J. Geophys. Res. **82**, 1985–2000, 1977

Dziewonski, A., Bloch, S., Landisman, H.: A technique for the analysis of transient seismic signals. Bull. Seismol. Soc. Am. **59**, 421–444, 1969

Forsyth, D.W.. The evolution of the upper mantle beneath mid-ocean ridges. Tectonophysics **38**, 89–118, 1977

Francis, T.J.G.. Upper mantle structure along the axis of the mid-Atlantic ridge near Iceland. Geophys. J. R. Astron. Soc. **17**, 507–520, 1969

Frank, F.C. Two-component flow model for convection in the earth's mantle. Nature **220**, 350–352, 1968

Gebrande, H., Miller, H., Einarsson, P. Seismic structure of Iceland along RRISP profile I. J. Geophys. **47**, 239–249, 1980

Girardin, N., Jacoby, W.R. Rayleigh wave dispersion along Reykjanes Ridge. Tectonophysics **55**, 155–177, 1979

Girardin, N., Poupinet, G. Teleseismic S travel-time delay for mid-Atlantic ridge earthquakes. Phys. Earth Planet. Inter. **9**, 306–313, 1974

Green, D.H., Liebermann, R.C. Phase equilibria and elastic properties of a pyrolite model for the oceanic upper mantle. Tectonophysics **32**, 61–92, 1976

Haigh, B.I.R. North Atlantic oceanic topography and lateral variations in the upper mantle. Geophys. J. R. Astron. Soc. **33**, 405–420, 1973

Hart, R.S., Press, F. Sn velocities and the composition of the lithosphere in the regionalized Atlantic. J. Geophys. Res. **78**, 407–411, 1973

Heirtzler, J.R., Dickson, G.O., Herron, E.M., Pitman, W.C., LePichon, X.· Magnetic anomalies, geomagnetic field reversals, and motions of the ocean floor and continents. J. Geophys. Res. **73**, 2119–2136, 1968

Heirtzler, J.R., LePichon, X., Baron, J.G.· Magnetic anomalies over the Reykjanes Ridge. Deep-Sea Res. **13**, 427–443, 1966

Keen, C.E., Fricker, A., Keen, M.J., Blinn, L.: Reykjanes Ridge crest studied by surface waves with the an earthquake-pair technique. J. Geophys. **47**, 265–270, 1980

McKenzie, D.P.: Some remarks on heat flow and gravity anomalies. J. Geophys. Res. **72**, 6261–6273, 1967

McKenzie, D.P., Bowin, C.: The relationship between bathymetry and gravity in the Atlantic ocean. J. Geophys. Res. **81**, 1903–1915, 1976

Orcutt, J.A., Kennett, B.L.N., Dorman, L.M.: Structure of the east Pacific rise from an ocean bottom seismometer survey. Geophys. J. R. Astron. Soc. **45**, 305–320, 1976

Parker, R.L., Oldenburg, D.W.: Thermal model of ocean ridges. Nature Phys. Sci. **242**, 137–139, 1973

Press, F.: Earth models consistent with geophysical data. Phys. Earth Planet Sci. Inter. **3**, 3–22, 1970

Ringwood, A.E.: Mineralogy of the mantle. In: Advances in earth science, P.M., Hurley, ed.: pp. 357–399. Cambridge, Mass. M.I.T. Press, 1966

RRISP Working Group: First results from Reykjanes Ridge Iceland Seismic Project 1977. Nature **279**, 56–60, 1979

Sclater, J.G., Francheteau, J.: The implications of terrestrial heat flow observations on current tectonic and geochemical models of the crust and upper mantle of the earth. Geophys. J. R. Astron. Soc. **20**, 493–509, 1970

Solomon, S.C.: Shear wave attenuation and melting beneath the mid-Atlantic ridge. J. Geophys. Res. **78**, 6044–6059, 1973

Solomon, S.C., Julian, B.R.: Seismic constraints on ocean-ridge mantle structure: anomalous fault plane solutions from first motions. Geophys. J. R. Astron. Soc. **38**, 265–285, 1971

Steinmetz, L., Whitmarsh, R.B., Moreira, V.S.: Upper mantle structure beneath the mid-Atlantic ridge north of the Azores based on observations of compressional waves. Geophys. J. R. Astron. Soc. **50**, 353–380, 1976

Talwani, M., LePichon, X., Ewing, M.: Crustal structure of the mid-ocean ridges, 2, computed model from gravity and seismic refraction data. J. Geophys. Res. **70**, 341–352, 1965

Talwani, M., Windisch, C.C., Langseth, M.G.: Reykjanes Ridge crest: a detailed geophysical study. J. Geophys. Res. **76**, 473–517, 1971

Vogt, P.R., Johnson, G.L.: Transform faults and longitudinal flow below the midoceanic ridge. J. Geophys. Res. **80**, 1399–1428, 1975

Weidner, D.J., Aki, K.: Focal depth and mechanism of mid-ocean ridge earthquakes. J. Geophys. Res. **78**, 1818–1831, 1973

Wyllie, P.J.: Role of water in magma generation and initiation of diapiric uprise in the mantle. J. Geophys. Res. **76**, 1328–1338, 1971

Yu, G.K., Mitchell, B.J.: Regionalized shear velocity models of the Pacific upper mantle from observed Love and Rayleigh wave dispersion. Geophys. J. R. Astron. Soc. **57**, 311–341, 1979

Received June 15, 1979; Revised Version September 10, 1979